



Denitrification, carbon and nitrogen emissions over the Amazonian wetlands

Jérémy Guilhen^{1,2}, Ahmad Al Bitar², Sabine Sauvage¹, Marie Parrens^{2,3}, Jean-Michel Martinez⁴,
Gwenaél Abril^{5,6}, Patricia Moreira-Turcq⁷, and José-Miguel Sanchez-Perez¹

¹Laboratoire Ecologie Fonctionnelle et Environnement (EcoLab), Institut national polytechnique de Toulouse (INPT), CNRS, Université de Toulouse (UPS), France

²Centre d'Observation de la Biosphère (CESBIO), CNES, Université de Toulouse (UPS), France

³Dynafor, Université de Toulouse, INRAE, INPT, INP-PURPAN, Castanet-Tolosan, France

⁴Géosciences Environnement Toulouse (GET), IRD/CNRS, Université Toulouse (UPS), France

⁵Biologie des Organismes et Ecosystèmes Aquatiques (BOREA), Muséum National d'Histoire Naturelle, Paris, France

⁶Programa de Geoquímica, Universidade Federal Fluminense, Outeiro São João Batista, Niterói, RJ, Brazil

⁷IRD (Institut de Recherche pour le Développement), GET (Géosciences Environnement Toulouse), UMR 5563, Lima, Peru

Correspondence: J. Guilhen (jeremy.guilhen@gmail.com) and S. Sauvage (sabine.sauvage@univ-tlse3.fr)

Abstract. In this paper, we quantify CO_2 and N_2O emissions from denitrification over the Amazonian wetlands. The study concerns the entire Amazonian wetland ecosystem with a specific focus on three focal locations: the Branco Floodplain, the Madeira Floodplain and the floodplains alongside the Amazon River. We adapted a simple denitrification model to the case of tropical wetlands and forced it by open water surface extent products from the Soil Moisture and Ocean Salinity (SMOS) satellite. A priori model parameters were provided by in situ observations and gauging stations from the HyBAm observatory. Our results show that the denitrification and emissions present a strong cyclic pattern linked to the inundation processes that can be divided into three distinct phases: activation - stabilization - deactivation. We quantify the average yearly denitrification and associated emissions of CO_2 and N_2O over the entire watershed at 17.8 kgN/ha/yr, 0.37 gC/m²/yr and 0.18 gN/m²/yr respectively. When compared to local observations, it was found that the CO_2 emissions accounted for 0.01% of the integrated ecosystem, which emphasizes the fact that minor changes to the land cover may induce strong impacts to the Amazonian carbon budget. Our results are quite consistent with the state of the art global nitrogen models with a positive bias of 28%. When compared to other wetlands in different pedo-climatic environments we found that the Amazonian wetlands have close emissions of N_2O to the tropical Congo wetlands and lower emissions than the tropical and temperate anthropogenic wetlands of the Garonne river, the Rhine river, and south-eastern Asia rice paddies. In summary our paper shows that a data driven approach can be successfully applied to quantify N_2O and CO_2 fluxes associated with denitrification over the Amazon basin. In the future, the use of higher resolution remote sensing product from sensor fusion or new sensors like the SWOT mission will permit the transposition to other large scale watersheds in tropical environment.



1 Introduction

Inland waters play a crucial role in the carbon and nitrogen cycle. In particular, wetlands are known to sequester the atmospheric and fluvial carbon (Abril and Borges, 2018). This phenomenon is intimately linked to nitrous oxide (N_2O) and carbon dioxide (CO_2) emissions to the atmosphere (Borges et al., 2015). In wetlands, during inundation periods denitrification processes
5 nitrates into atmospheric dinitrogen that sustains emissions of N_2O and CO_2 . These processes are controlled by biogeochemical reactions linked to micro-organisms activity and pedoclimatic conditions (soil characteristics, nutrients availability and water content). Moreover the alternations between terrestrial and aquatic phases in wetlands promotes carbon and nitrogen mineralization and denitrification in soils (Koschorreck and Darwich, 2003). Our understanding and capacity to quantify the mechanisms involved in N_2O and CO_2 emissions over wetlands are limited which leads to uncertainties in estimating them at
10 large scales.

During the last decade, process-based models have become paramount tools in estimating carbon and nitrogen budgets in the context of global multi-source changes. Recent studies presented a review of existing models capable of quantifying N_2O and CO_2 fluxes over continental ecosystems (Tian et al., 2018; Lauerwald et al., 2017). They are mainly used to characterize the part of greenhouse gases (GHGs) emissions due to natural and anthropogenic/agricultural activities at different spatial-temporal
15 scales. The estimation of N_2O emissions from natural sources are still subject to large uncertainties (Ciais and Coauthors., 2013) while N_2O emissions from anthropogenic activities are under investigations. Assessing N_2O budget for wetlands at large scale currently constitutes a knowledge gap. In terms of denitrification, the relatively sparse and short-term observations limits our capability to estimate the carbon and nitrogen recycling in terrestrial ecosystems, especially over wetlands. Since in situ measurements constitute the main source of data, few studies assess N_2O and CO_2 emissions from denitrification at large
20 scale and are usually limited to field scale or small scale watersheds (Russell et al., 2019; Johnson et al., 2019; Korol et al., 2019).

In the case of the Amazon basin, the total amount of CO_2 emission reaches 0.3 PgC/yr for both natural and agricultural sources. Scofield et al. (2016) pointed out over the Amazonian wetlands the disproportionally high CO_2 out-gassing may be explained by the abundant amount of podzols for the Negro Basin. Those types of soils are likely to slow organic matter
25 decomposition and increase leaching of humus. Elsewhere over the Amazon, floodplain soils are mainly Gleysols (Legros, 2007) which are characterized by a high microbiological activity. CO_2 emissions from the river are mainly due to organic matter respiration as well as exports from the wetland system. In wetland, root respiration and microbial activities are a major source of CO_2 emissions (Abril et al., 2014). Ultimately CO_2 outgassed from the Amazon River is about 145 ± 40 TgC/yr (de Fatima F. L. Raseira et al., 2008) and tops at 470 TgC/yr when extrapolated to the whole basin (Richey et al., 2002). How-
30 ever, considering the carbon budget, it is not clear to which extent the Amazon basin acts as a sink of carbon. Some studies show that the Amazon basin is more or less in balance and even acts as a small sink of carbon at the amount of 1GtC/yr (Lloyd et al., 2007). Remote sensing have emerged as an essential tools for GHGs quantification, either via assimilation into physically-based models (Engelen et al., 2009) or as a direct observation (Bréon and Ciais, 2010). For wetlands the monitoring of water extents is crucial for the denitrification processes. Water surface monitoring has been done with a variety of spectral



bands (Martinez and Le Toan, 2007; Pekel et al., 2016; Birkett et al., 2002) in active and passive remote sensing. Recently L-Band microwave remote sensing showed advanced capabilities to monitor water surfaces in tropical environment because of all-weather capabilities, providing soil signal under vegetation (Parrens et al., 2017).

This study aims at delivering an enhanced understanding and quantification of the denitrification process over Amazonian wetlands with their associated fluxes of N_2O and CO_2 using modelling and microwave remote sensing. We constrained and adapted denitrification process-based set of equations by L-Band microwave water surface extents from the SMOS satellite and a priori information from in situ. The specific objectives of the study are to highlight the main key factors controlling the denitrification and to provide the hot-spots and hot-moments of denitrification over wetlands.

2 Materials and methods

2.1 Study area

The Amazon basin (Fig.1) is the world largest drainage basin with an area of $5.5 \times 10^6 \text{ km}^2$ and an average water discharge of $208\,000 \text{ m}^3 \text{ s}^{-1}$ (Callode et al., 2010) representing 20% of all freshwaters transported to the ocean. The watershed spans across Bolivia, Colombia, Ecuador, French Guiana, Peru, Suriname, and Guyana and 68% of the basin pertains to Brazil. The Amazon

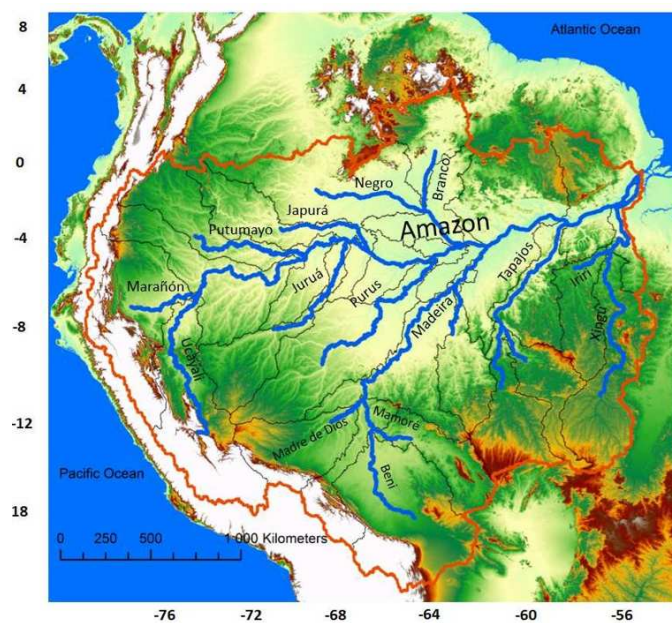


Figure 1. The Amazon basin and its main tributaries.

hydrology is governed by three main sources: the Andes, the Brazilian and Guyana shields and the lowlands. Devol et al. (1995) described the hydrology of the main stream as the aggregation of the water originating from Andean regions, from the main tributaries and from “local sources” corresponding to smaller streams draining local lowlands. The contribution of each water



body differs in time. For example from November to May the contribution of Andean waters reaches 60% and declines during the dry season to 30%. Wetlands are paramount in the watershed functioning : 30% of the Amazon discharge has once passed through the floodplain (Richey et al., 1990) alongside a 2010 km long reach between São Paulo de Olivença and Óbidos (Bourgoin et al., 2007). The Amazon watershed can be divided into 8 major sub-basins: (1) the Negro basin, (2) the Branco basin, (3) the Solimoes River and its tributaries, (4) the Madeira basin, (5) the Purus basin, (6) the Tapajós basin, (7) the Xingu basin and (8) the section between Manaus and the mouth of the Amazon River. We used that delineation when we designed our model (Fig. 3) as it represents the main hydrosystems of the Amazon basin.

The Amazon basin contains several floodplains. Here we consider the three main floodplains: the Branco floodplain in the northern part, the Madeira floodplain in the southern part and the floodplain between Óbidos and Manaus which is called Obidos - Manaus floodplain (O-M FP) in the following. The O-M FP covers an area of 2.5×10^5 km² whereas the Madeira floodplain covers 3.7×10^5 km². The Branco floodplain is the widest of the three floodplains with a covered area of 6.7×10^5 km².

2.2 In situ data from the HyBAM observatory

In situ data and gauging stations data were obtained from the HyBAM international network (www.ore-hybam.org). Hybam stems from the precedent PHICAB and HiBAM projects in Bolivia and Brazil. The main objective of this network is to monitor the hydrology, geochemistry and sediment load of the main Amazonian rivers with associated quality and uncertainty. The French Research Institute for the Development (IRD) the Water National Agency (ANA), the University of Brasilia (UnB) and the Federal University of Amazonas at Manaus (UFAM) contribute to the HyBAM observatory. Gauging station discharges and DOC values of the main tributaries were extracted from the HyBAM monitoring data base.

20

2.3 Water surface extents from L-Band microwave

The Soil Water Fraction (SWAF) retrieved from L-Band microwave are used to determine the open water surfaces (Parrens et al., 2017). SWAF is obtained using a contextual model to the Soil Moisture Ocean Salinity (SMOS) angle binned brightness temperatures (MIRCLF3TA) (Al Bitar et al., 2017). SMOS launched in November 2009 by the European Space Agency (ESA), was the first dedicated soil moisture mission. SMOS is a passive microwave 2-D interferometric radiometer operating in L-band (1.413 GHz, 21 cm wavelength) (Kerr et al., 2010). SMOS orbits at a 757 km altitude and provides brightness temperature emitted from the Earth over a range of incidence angles (0° to 55°) with a spatial resolution of 35 to 50 km. Parrens et al. (2017) showed the capability of SMOS to retrieve the water fraction under dense forests over the Amazon basin. One of the main upsides of SMOS is its sensitivity to soil signal under vegetation in all-weather conditions thanks to the L-Band frequency. The SWAF data was averaged each month over the sampling period (2011 - 2015) within the Amazon basin. Fig.2 shows the average of the SWAF computed over the full period at V-polarization and at $32^\circ \pm 5^\circ$. It outlines the common hydrological pattern observed in the Amazon basin as well as the dynamic of the inundations for the different floodplains.

30

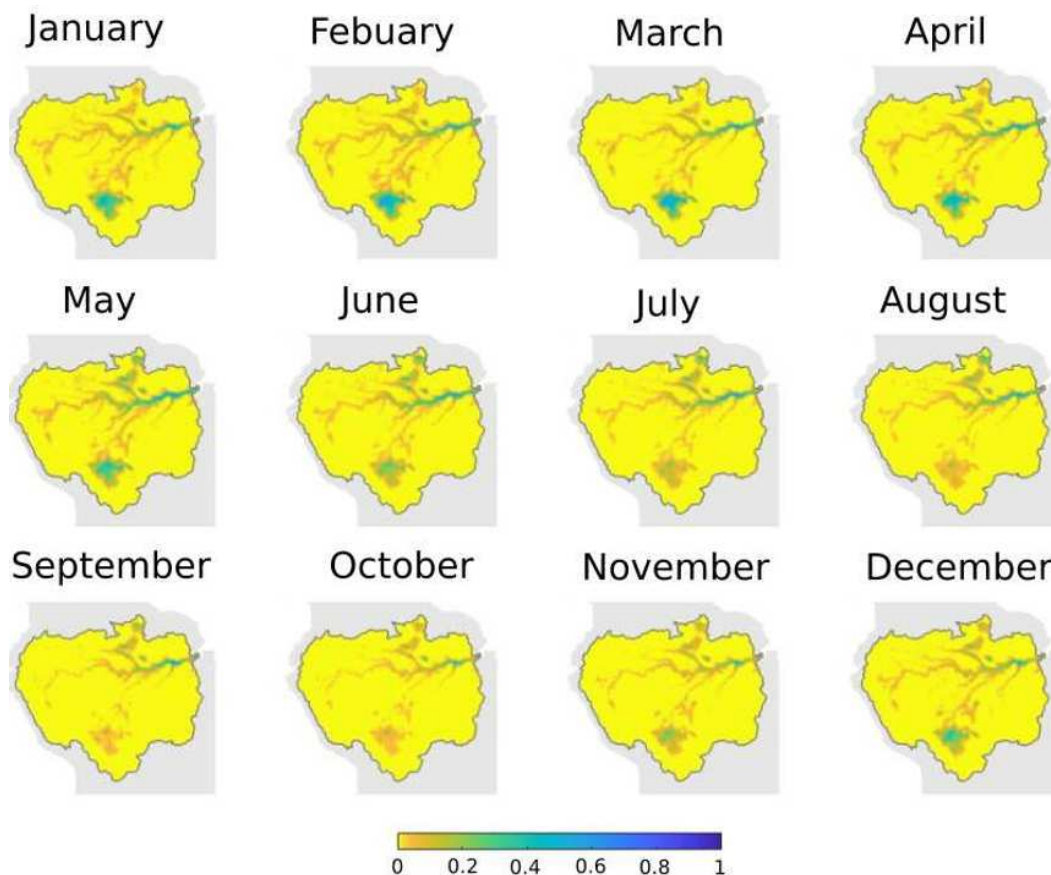


Figure 2. Monthly average of the SWAF product from 2011 to 2015 at V-polarization and 32. It represents the seasonal evolution water bodies and extents through the year within the basin.

2.4 Methods

2.4.1 Assessing denitrification and out-gassing

In this study, we modified the denitrification rate proposed by Peyrard et al. (2010) to fit tropical wetland conditions. Denitrification is a consumption of dissolved organic carbon (DOC), particulate organic carbon (POC) and nitrate (NO_3^-) in soil limited by dioxygen (O_2) and ammonium (NH_4^+) availability. Here, because denitrification is regarded as occurring during flooding events while the soil is saturated and extremely low oxygen is available, we consider that O_2 is not a limiting factor (Dodla et al., 2008). Furthermore, as there is only one flooding event over the watershed per year over the particularly active Amazonian ecosystem, it is supposed that all the ammonium is processed into nitrate between two consecutive floods. Thus, we also supposed that NH_4^+ is not limiting neither. The fact that nitrate stocks are reconstituted under aerobic conditions, e.g. when soils are no longer flooded, is a reasonable assumption in the case of the Amazon basin and more particularly for the



wetland parts (Hulme, 2005; Brettar et al., 2002). Besides, many studies consider denitrification as a combine consumption of nitrates and carbon (Scofield et al. (2016); Dodla et al. (2008); Goldman et al. (2017)). Taking into consideration the above statements, the denitrification rate can be expressed as:

$$R_{NO_3} = -0.8 \cdot \alpha \cdot \left(\rho \cdot \frac{1 - \phi}{\phi} \cdot k_{POC} \cdot [POC] \cdot \frac{10^6}{MC} + k_{DOC} \cdot [DOC] \right) \cdot \frac{[NO_3]}{k_{NO_3} + [NO_3]} \quad (1)$$

- 5 where R_{NO_3} is the denitrification rate in $\mu\text{molL}^{-1} \text{d}^{-1}$, $0.8 \cdot \alpha$ represent the stoichiometric proportion of nitrate consumed in denitrification compared to the organic matter used with $\alpha = 4$ as mentioned in Peyrard et al. (2010), ρ is the dry sediment density kgdm^{-3} , ϕ is the sediment porosity, k_{POC} is mineralization rate constant of POC (d^{-1}), POC is the Particulate Organic Carbon content in the soil and the aquifer sediment (1 per thousand), MC is the carbon molar mass g mol^{-1} , DOC is the concentration of Dissolved Organic Carbon (DOC) in the aquifer water μmolL^{-1} , k_{DOC} is the mineralization rate constant of DOC (d^{-1}), k_{NO_3} is the half-saturation for nitrate limitation in μmolL^{-1} and NO_3 is nitrate concentration in the aquifer in μmolL^{-1} .

- 15 Estimation of out-gassing CO_2 is based on the denitrification equation where gaseous CO_2 is formed. It is supposed that neither nitrates nor organic matter are limiting factors for the reaction which is considered total (eq. 2) (de Freitas et al., 2001). Abril and Frankignoulle (2001) showed that denitrification tends to raise the alkalinity. In order to take into account this phenomenon, the formation of HCO_3^- from dissolved CO_2 (eq. 3) was coupled to the denitrification (eq. 2). Overall, in this study, denitrification was modelled using:



- 20 The equation of the chemical reaction of denitrification (eq. 4) is used to determine the generated amount of CO_2 by relating it to the amount of denitrified NO_3 . Finally, N_2O production is indirectly estimated as a result of N_2 formation and the ratio was set to 0.1.



2.4.2 Parametrization of dissolved/particulate organic carbon and nitrate concentrations

- 25 The model parameters for the denitrification are taken from references studies and in situ measurements. The sediment porosity ϕ was set to 25%. k_{POC} , k_{DOC} and k_{NO_3} were set to $1.6 \times 10^{-5} \text{d}^{-1}$, $1 \times 10^{-3} \text{d}^{-1}$ and $1.0 \times 10^{-6} \mu\text{molL}^{-1}$ respectively. Nitrate concentrations (NO_3^-) were considered constant over the period. As the Amazon is one of the most active region of the world (Legros, 2007) in term of microbial soil dynamic, it was assumed that on the one hand, during non-flooding period, mineralization of nitrogen was sufficient to compensate nitrate loses by plant assimilation and leaching. On the other hand, during flooding period and for inundated soils, when denitrification is triggered, nitrate inputs from streams were abundant enough to sustain this process (Sánchez-Perez et al., 1999). For POC concentration, according to the studies performed by



Moreira-Turcq et al. (2013), it was considered constant over the whole watershed and for the global period of the simulation (2011 – 2015) to 1 %. The HyBAM database provides measurements of *DOC* both over time and for few streams. Dissolved organic carbon concentration in streams is highly correlated to discharge (Ludwig et al., 1996). The stable seasonality over time of the Amazonian streams was demonstrated by prior studies (Paiva et al., 2013). Considering these two properties, streams were regrouped regarding the main sub-basins of the Amazon watershed mentioned in Section 2.1. For each sub-basin, the average monthly discharge was calculated using the HyBAM's gauging station's records. We then used those discharge tendencies to extrapolate the average monthly *DOC* concentration based on in situ records (figure 3). It was supposed that there is no difference for the *DOC* value between the different years.

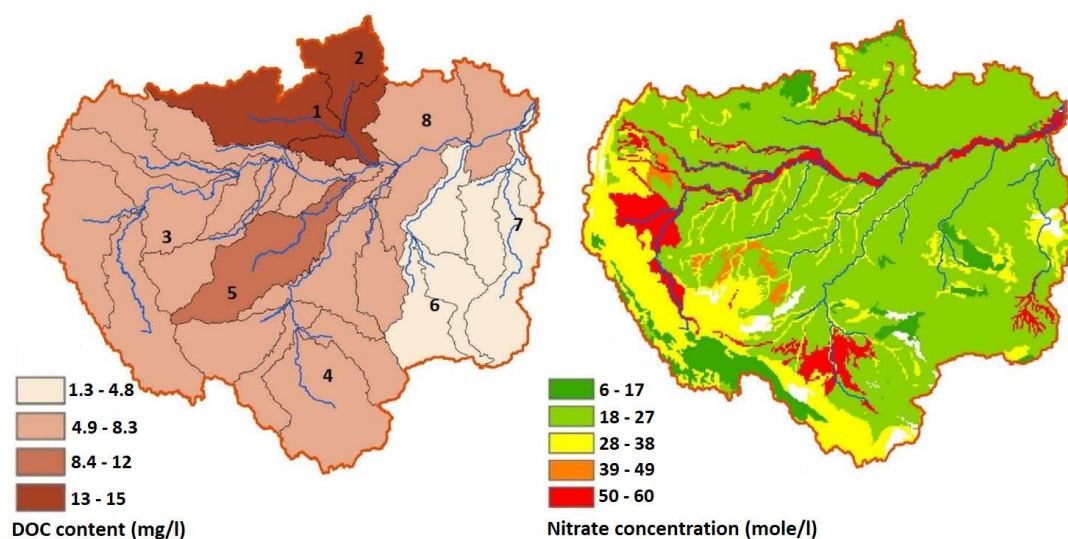


Figure 3. Map of spatial parameters of the model. (Left) DOC contents of the main streams in January 2011. The values are given in mg/L. As a matter of convenience, this values are depicted for the associated sub-basin. The main sub-basins are easily distinguishable by having different shades. (Right) Spatial representation of the nitrate contents of the watershed for each types of soil. Values are given in mole/l

2.4.3 Denitrification computation

The methodology focuses on modelling the denitrification process that occurs in the first 30 cm of water-saturated soils in wetland. Thereby, only the nitrates included in that layer were considered undergoing denitrification. Nitrates brought by streams are supposed not to modify significantly the amount of nitrates contained in the soil solution. Indeed, the concentration of nitrates in the river is negligible to the concentration of riverine aquifers (Sánchez-Pérez et al., 2003). We consider that the *DOC* in the soil is directly brought by streams so the amount of *DOC* included in soils is set up to the streams values. Most of the organic carbon is transported from alluvial sediments or brought by streams during flooding events (Peter et al., 2012). We consider that the gases produced during the denitrification are entirely emitted to the atmosphere regarding the supersaturation



of pCO_2 in groundwater (Davidson et al., 2010). Overall, denitrification was calculated as:

$$D_{NO_3} = R_{NO_3} \cdot SWAF \cdot Q_{wa} \quad (5)$$

where D_{NO_3} is the net denitrification in *mole/month*, R_{NO_3} is the denitrification rate in *mole/month/L*, SWAF is the fraction of land covered with open waters and Q_{wa} is the water storage capacity for each type of soil (*L*). Soil data were determined from the Food and Agricultural Organization (FAO) database. The soil description file, constituted of thousands of soils, was summed up into 36 categories accordingly to soil textures and an associated nitrate concentration limit was given (figure 3). In summary the model requires the inputs and parameters for : (1) the types of soil and their nitrogen contents in order to assess the base pool of nitrates, (2) the dissolved organic carbon concentrations of the streams that overflow and (3) the extent of inundated surfaces. The model was applied at daily scale from January 1st 2011 to December 31th 2015 and monthly maps were then generated. Note that in order to assess the denitrification only occurring in wetlands, the minimum SWAF value recorded during the period (2011 - 2015) is subtracted to each month simulation, as it accounts as a residual artefact of streams.

3 Results

3.1 Spatial and temporal patterns of denitrification over the Amazon Basin

Denitrification and emissions of CO_2 , N_2O and N_2 are simulated for each months from 2011 to 2015. Figure 4 shows the yearly average maps of denitrification, CO_2 and N_2O emissions over the Amazon Basin. The three major hot spots which correspond to the major floodplains of the Amazon Basin are identified.

Figure 5 presents the monthly denitrification, CO_2 and N_2O emissions over the Amazon Basin from 2011 to 2015. The denitrification process leads to similar temporal patterns of CO_2 and N_2O at basin scale. From November to March denitrification and emissions become active with the increase of nitrates denitrification in the Basin. During the first months, until December, the activation is slow and mild. It then increases in the following months and peaks in March at 1.16×10^9 kg of N- NO_3 denitrified, 2.15×10^8 kg of C- CO_2 , 1.0×10^8 kg of N- N_2O . Between March and June, denitrification and emissions are steady and fluctuate respectively around 9.51×10^8 kg of N- NO_3 denitrified, 2.04×10^8 kg of C- CO_2 , 9.51×10^7 kg of N- N_2O . Finally it is observed from June to October that the processes inactivates at a slower rate (-33%) than activation. Subsequently, the decreasing trend shifts and tops in August. Values registered in September are lower than in August, and yet in year 2011, 2012 and 2015, these were fairly close. The decreasing trend reaches eventually a minimum peak in November at 1.96×10^8 kg of N- NO_3 denitrified, 4.20×10^7 kg of C- CO_2 , 1.96×10^7 kg of N- N_2O .

The mean annual denitrification and emissions represent the main trends observed over the watershed. Additionally, it shows more precisely three hot moments in March, June and August of each year. The first two hot moments, in March and June, are maximum area peaks. During these months, in spite of observing a low activity over the watershed (below 8.7×10^5 kg of N- NO_3 denitrified per pixel, the extent of surfaces undergoing denitrification is the highest. On the contrary, the August hot moment is mainly due to a particularly strong denitrification between Obidos and Manaus with peaks of 6.16 and 7.2×10^6 kg

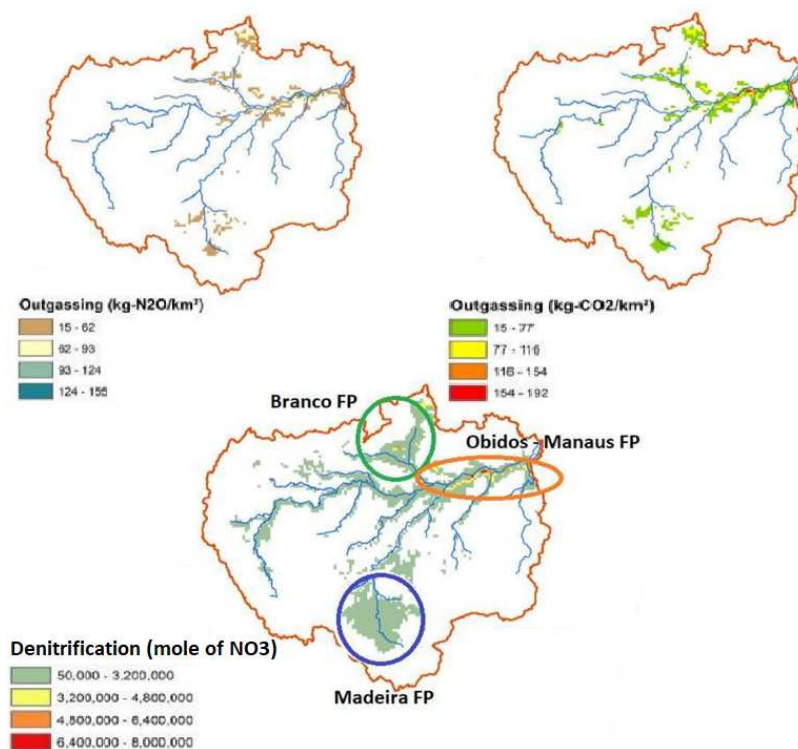


Figure 4. Spatial representation of N_2O , CO_2 and denitrification summed over the year 2011 to year 2015. The Denitrification shows the main floodplains that were isolated in the the study.

of $N-NO_3$ denitrified. CO_2 emissions average 1.75×10^8 kg of $C-CO_2$ per month over the basin. N_2O emissions fluctuate around 6.52×10^7 kg of $N-N_2O$ out-gassed per month from the watershed.

3.2 Focus on the main three Amazonian floodplains

The temporal patterns of the processes over the entire basin and throughout the whole period are unique in each floodplain. In fact, the three floodplains do not become active/ inactive at the same time and do not reach their maximum potential activity at the same moment either. Figure 6 shows the monthly behaviour of denitrification, CO_2 and N_2O emissions for each floodplain together with the respective one over the entire basin. The following comments can be given:

- The Obidos - Manaus floodplain follows the same pattern as the global trend and is mainly active between March and June but it never becomes totally inactive during the October – December period. It undergoes an average denitrification of 2.2×10^8 kg of $N-NO_3$ and emissions of 4.78×10^7 kg of $C-CO_2$ and 2.23×10^7 kg of $N-N_2O$.
- The Madeira floodplain follows the O-M FP's same pattern. However, it becomes active in October and on average reaches its maximum in March with 2.93×10^8 kg of $N-NO_3$ denitrified, 6.28×10^7 kg of $C-CO_2$, 2.93×10^7 kg of

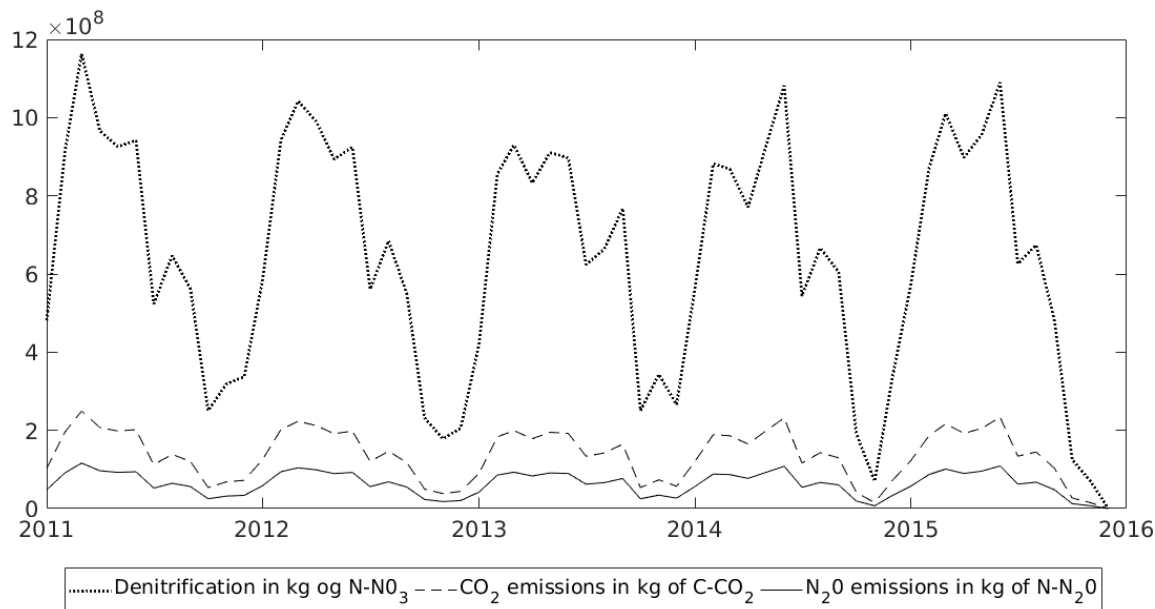


Figure 5. Monthly denitrification (dots), CO_2 (dashes) and N_2O (line) emissions over the watershed for the period 2011 - 2015. Values are given in kg of Nitrogen and Carbon.

$N-N_2O$. The processes intensity decrease fast after. A top peak is usually observed afterwards in June at 3.03×10^8 kg of nitrate denitrified, 6.49×10^7 kg of $C-CO_2$ and 3.03×10^7 kg of $N-N_2O$. The Madeira floodplain is almost inactive with a low denitrification and emissions occurring between July and October below 5.17×10^7 kg of $N-NO_3$ denitrified, 1.11×10^7 kg of $C-CO_2$ and 5.17×10^6 kg of $N-N_2O$.

- 5 – The Branco floodplain is the less constant of the three floodplains even though a general pattern can be observed. The floodplain becomes active in January but the activation is slow and the denitrification is low until April (less than 1.7×10^8 kg of $N-NO_3$ as well as the emissions of 4.0×10^7 kg of $C-CO_2$ and 1.70×10^7 kg of $N-N_2O$). Afterwards, the processes increase more importantly and tops in May (2011, 2012, 2013) / June (2014 and 2015) and September 2013
- 10 October to February/March with denitrification and emissions barely reaching 1.20×10^8 kg of $N-NO_3$ and 2.50×10^7 kg of $C-CO_2$, 1.20×10^7 kg of $N-N_2O$ respectively.

The detailed functioning of each floodplain explains the general pattern observed for the processes. The O-M FP drives the general trends of the total denitrification, CO_2 and N_2O emissions of the watershed and the three different phases: activation, fluctuation and inactivation. The March peak is mainly due to the Madeira floodplain reaching a maximum of activity. The

15 June peak happens for the same reason in year 2011, 2012 and 2013. In 2014 it is due to the combined effect of the Branco and

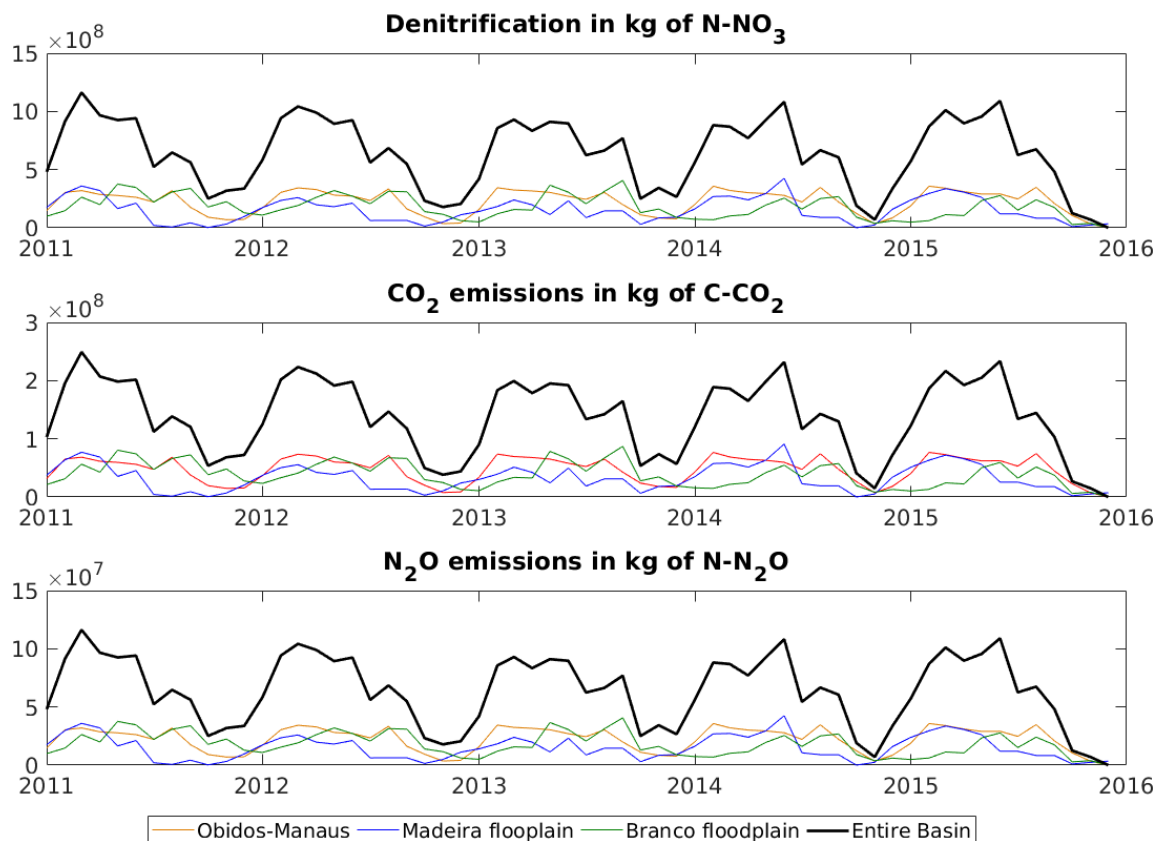


Figure 6. Monthly time series of denitrification (top), CO_2 emissions (middle) and N_2O emissions (bottom) over the period (2011-2015). The black line represents the whole Basin denitrification, the green line corresponds to the denitrification over the Obidos - Manaus floodplain, the red line depicts the denitrification over the Madeira floodplain and the blue line the denitrification over the Branco floodplain

the Madeira floodplain topping activities whereas in 2015 only the Branco floodplain is contributing. The August peak is due to the rising of the O-M FP and the Branco floodplains activity again.

Figure 7 presents the monthly contribution of each floodplain to the global denitrification pattern. Overall, the three floodplains contribute to 80% of the Basin denitrification. From January to March it is mainly supported by the O-M and the Madeira floodplains, whereas from July to November it is due to the O-M and the Branco activity. In April, May, June and December the involvement of the floodplains is similar. While, the O-M floodplain constitutes the main source of denitrification of the watershed, the Branco and the Madeira floodplains contribute similarly to the process and at a lower extent (p.value = 1.35×10^{-8} , ANOVA). The same conclusions are equivalent for the CO_2 and N_2O emissions.

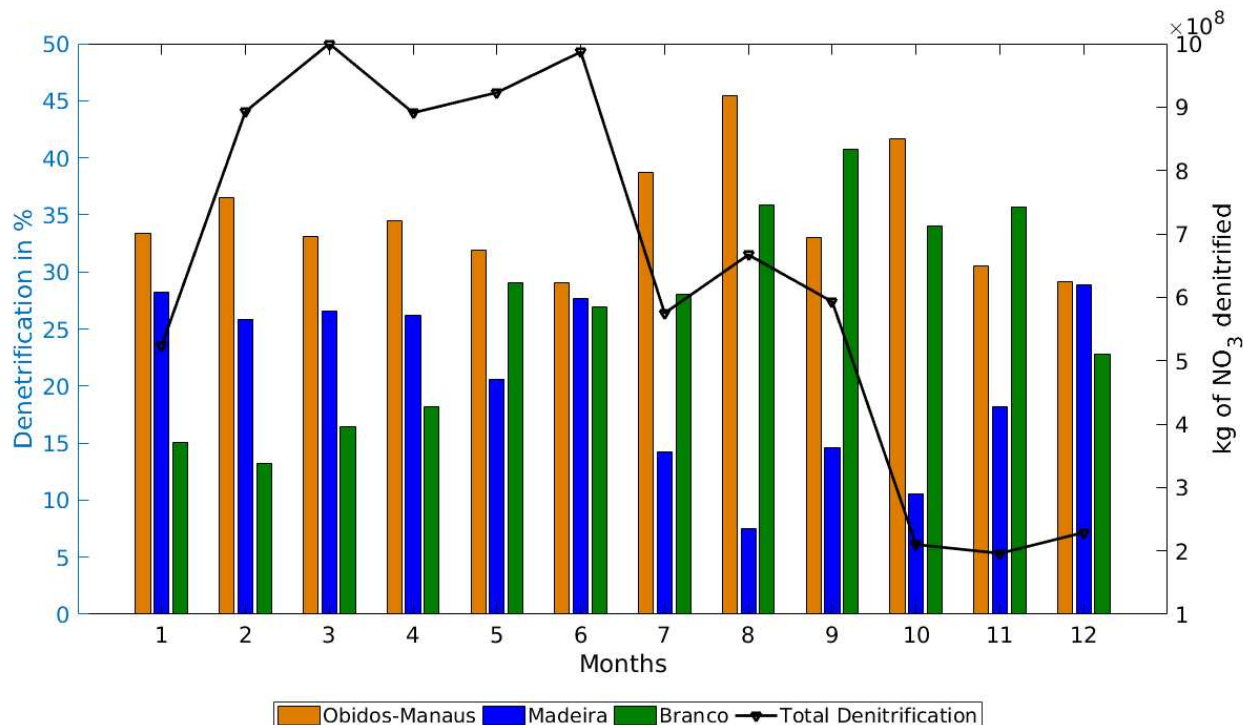


Figure 7. Average monthly contribution of each floodplain to the Basin denitrification, the blue bar represents the denitrification over the Obidos - Manaus floodplain, the green bar over the Madeira floodplain and the yellow bar the denitrification over the Branco floodplain. The monthly average denitrification (black line) results from the three floodplains.

3.3 Emissions of greenhouse gases from the Amazonian wetlands

Table 1 depicts the yearly emissions of CO_2 and N_2O over the Amazon basin and the three main floodplains. Emissions of CO_2 from denitrification are twice as much higher than N_2O emissions over the basin. Averagely, flooded areas emits 2.76×10^9 kg C- CO_2 per year and 1.03×10^9 kg N- N_2O per year by denitrification from the natural nitrate pool of the watershed.

Wetland	Area (ha)	CO_2 (kgC)	N_2O (kgN)	N_2 (kgN)
Amazon basin	5.7×10^8	$1.1 \times 10^{10} \pm 2.75 \times 10^8$	$1.03 \times 10^9 \pm 2.57 \times 10^7$	$1.03 \times 10^{10} \pm 2.57 \times 10^8$
Obidos - Manaus FP	2.5×10^7	$3.82 \times 10^9 \pm 9.94 \times 10^7$	$3.56 \times 10^8 \pm 9.28 \times 10^6$	$3.56 \times 10^9 \pm 9.28 \times 10^7$
Madeira FP	3.7×10^7	$2.40 \times 10^9 \pm 2.65 \times 10^8$	$2.24 \times 10^8 \pm 2.47 \times 10^7$	$2.24 \times 10^9 \pm 2.47 \times 10^8$
Branco FP	6.78×10^7	$2.79 \times 10^9 \pm 6.17 \times 10^8$	$2.6 \times 10^8 \pm 5.75 \times 10^7$	$2.6 \times 10^9 \pm 5.75 \times 10^8$

Table 1. Average yearly CO_2 emissions in kgC- CO_2 , N_2O emissions in kgN- N_2O and N_2 emissions in kgN for the Amazon basin and the three main floodplains.



Over the observation period, it appears that the emissions of CO_2 and N_2O over the whole basin are steady with no significant change from 2011 to 2015. During that period, the O-M FP is the floodplain which contributes the most to the emissions for the both gases and its activity remains equivalent. However, in 2014 the dynamics of the Madeira and the Branco FP changed. Indeed from 2011 to 2013, the Branco FP roughly emitted twice as much gases than the Madeira FP. This trend shifted in 2014 with the involvement of the Madeira FP becoming more important in term of emissions than the Branco FP. At a yearly basis, the whole Amazon Basin undergoes a denitrification of about 1.03×10^{10} kgN/ha/yr.

3.4 Denitrification and gazes emissions anomalies

During the period of the study, major meteorological events were recorded over the Basin. On one hand, year 2011 was a “La Niña year”. La Niña periods leads to wetter weather conditions in South America. From October 2013 to March 2014, peculiar heavy rainfalls were documented on the Madeira regions and caused extreme flooding in this region and nearby Obidos. It was supposed that these two events might have had an enhancing effect on denitrification and thus on gas emissions. On the other hand, September 2015 marked the beginning of an El Niño episode that carried on after the study. In South America and the Amazon, El Niño is likely to produce drier weather conditions which reduces the intensity of the denitrification and the microbiological processes.

Fig.8 shows the monthly anomalies of denitrification observed over the Amazon watershed from 2010 to 2015. Anomalies were calculated by subtracting the value of a month to the average value of the same month. Positive anomalies show an intense denitrification whereas negative abnormalities show a denitrification lower than the average. Examining the anomalies of the watershed and the floodplains shows that during La Niña year most of the abnormalities are positive especially for the first months. However during El Niño episode, all the abnormalities are negative. El Niño is the only meteorological event that has a significant effect on the processes (p.value= 4.4×10^{-3}). Moreover it impacts the three floodplains (p.value= 3.43×10^{-4}). Months undergoing the El Niño episode show a reduction of 27.7% than average values.

It appears that extreme events do not have an uniform impact on the whole basin. Table 2 sums up the spatial denitrification for the Amazon basin and the three floodplains at a yearly scale. Overall denitrification may not be impacted at watershed scale. The average denitrification rate for the whole basin shows little inter annual variations. However, in 2015 simulated denitrification for the Branco FP was twice as low than for the year 2011. As so, it can be assumed that this floodplain has been drying off during the 2011 - 2015 period and thus is much more sensitive to drier conditions than other parts of the watershed.

Table 2. Yearly denitrification for the whole basin and the major three floodplains from 2011 and 2015. Values are given in kgN/ha/yr.

Denitrification (kgN/ha/yr)	2011	2012	2013	2014	2015
Basin	18.4	18.0	17.9	17.5	17.2
O-M FP	137.3	140.6	144.9	146.9	142.7
Madeira FP	57.4	56.3	53.3	67.4	67.7
Branco FP	48.5	43.0	43.0	31.4	28.3

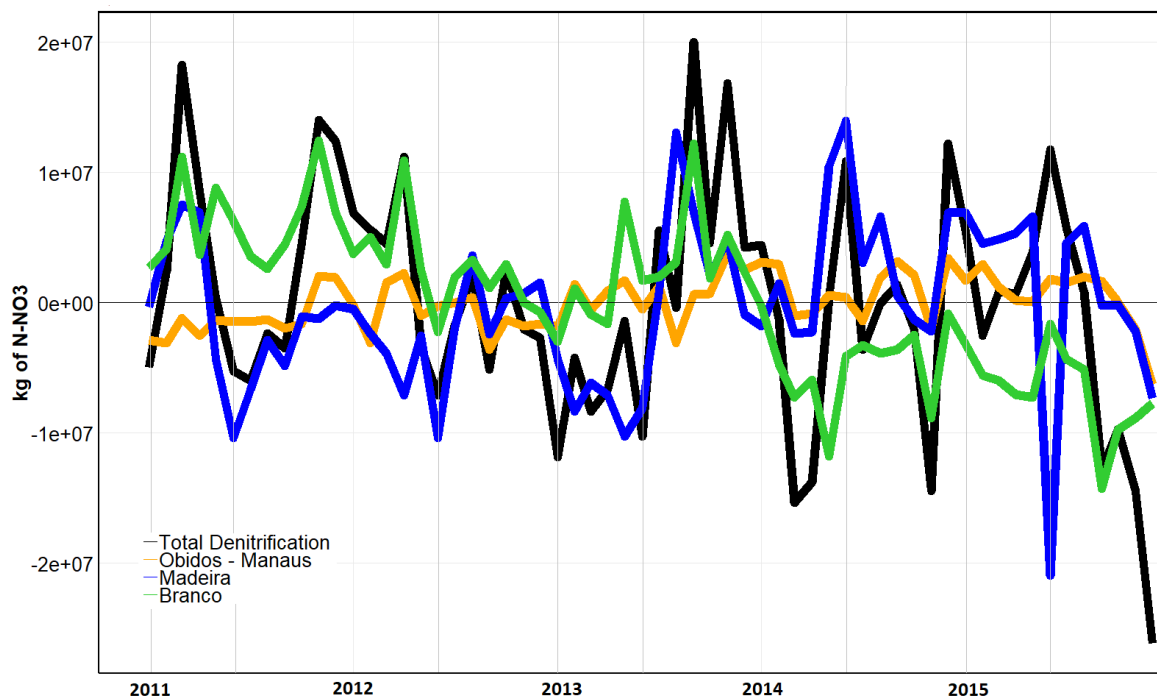


Figure 8. Monthly anomalies at the basin and main floodplains scale for denitrification throughout the period (2011-2015). The blue line represents the basin denitrification, the orange line refers to the denitrification of the O-M FP, the grey line is for the denitrification over the Madeira FP and the yellow line is the denitrification over the Branco FP.

4 Discussion

4.1 Determining key factors of the denitrification

A sensitivity analysis of the parameters of the denitrification equation (1) was performed. k_{poc} can range from 0.15×10^{-6} to 1.1×10^{-4} which leads to a yearly denitrification 46% lower and 18% higher than the initial values respectively. k_{doc} range from 1.0×10^{-4} to 1.22 which leads to values of denitrification 94% lower and $1.333 \times 10^5\%$ higher respectively. It follows that for the Amazon Basin k_{doc} is evaluated as more sensitive than k_{poc} . Also, the nitrates related part of the denitrification equation was analysed analytically. Nitrates are relatively abundant in the watershed's soils and it is noticeable that k_{NO_3} is negligible compared to NO_3 though $\lim_{NO_3 \rightarrow \infty} \frac{[NO_3]}{k_{NO_3} + [NO_3]} = 1$. It appears that nitrates may be a non-limiting factor of denitrification for the Amazon basin. Overall, the denitrification equation currently depends on four variables: POC, DOC and NO_3 and SWAF. NO_3 and POC appear to be non-limiting factors of the denitrification equation.

Table 3 depicts for the O-M, Madeira and Branco floodplains the effective denitrification over the 2011 - 2015 period in kgN/ha/yr as well as the average and standard deviation values of DOC concentration in mg/L and SWAF index. The denitrification values show that all the three floodplains are particularly active systems in term of processing. The Branco floodplain,



which is the bottom value of the set with an average potential of 38.8 kgN/ha/yr, has values at least twice as much higher than natural ecosystems. The O-M floodplain is an active floodplain in term of denitrification potential with an average annual intensity of 142.5 kgN/ha/yr. The *DOC* show that the Branco is the highest floodplain in terms of *DOC* concentration with an average of 8.93 ± 2.87 mg/L, followed by the O-M with 5.65 ± 2.45 mg/L and the Madeira floodplain 2.26 ± 2.45 mg/L.

5 Similar to the *DOC*, the average and standard deviation of the SWAF values were extracted from the daily observations over the 2011 - 2015 period. The ranked order of the floodplains for the SWAF component is similar to the denitrification one. This result strengthens the importance of sensing waterbodies and that our model is driven by inundated surfaces patterns and intensities. Eventually, the differences of denitrification intensity observed for the three floodplains are the combined effect of the variations of the *DOC* concentrations and the SWAF. As a matter of facts, *DOC* assesses the average maximum denitrification

10 rate of a floodplain. Whereas the SWAF value is the main driving factor of the model which reveals the actual denitrification. Overall, the actual denitrification rate (equation 1) may be improved as a combination of a potential rate function (provided by *DOC* and *POC*) and limitation functions provided by the peculiar environmental conditions.

Table 3. Overall denitrification in kgN/ha/yr, mean and standard deviation of the SWAF and DOC (mg/L) values for the three floodplains

Floodplain	Denitrification	DOC		SWAF	
		Mean	Standard deviation	Mean	Standard deviation
Obidos - Manaus	142.5 kgN/ha/yr	5.65 mg/L	2.45 mg/L	3.3%	0.12%
Branco	38.8 kgN/ha/yr	8.93 mg/L	2.87 mg/L	1.4%	0.27%
Madeira	60.4 kgN/ha/yr	2.26 mg/L	2.45 mg/L	1.7%	0.17%

4.2 Comparing to physically-based models

The N_2O emissions at large scale are compared to results to the NMIP project (Tian et al., 2018) model, more particularly

15 DLEM (Xu et al., 2017), VISIT (Ito and Inatomi, 2012) and O-CN (Zaehle and Friend, 2010). These models consider the N_2O emissions from nitrification and denitrification, where in our case only denitrification during flooding is considered as nitrification is mainly used for refilling the nitrogen pool. Also the aggregate impact of temperature, water saturation of the soil, nitrogen contents, soil pH and micro-organisms activity, explicitly modelled in the physically based models, is accounted for in our approach through the parameters k_{POC} and k_{DOC} and mineralisation rate included in equation (1) ((Peyrard et al., 2010;

20 Sun et al., 2017).

During the period 2011 - 2015 those models evaluated emissions of N_2O from the Amazon basin at about 0.14 gN/m²/yr. Our model simulates emissions of N_2O at roughly $0.18 \pm 4.4 \times 10^{-3}$ gN/m²/yr over the basin. The peculiar emission of the 1.3×10^{11} m² wetlands system represent 0.81 ± 0.02 gN/m²/yr. We can observe that our model gets a global higher estimation of the emissions of N_2O at a rate of 28% than the other models with 80% of them (0.14 gN/m²/yr) originates from the three

25 main floodplains; the Obidos - Manaus, the Madeira and the Branco. In term of input data, our model as well as DLEM, VISIT and O-CN use climate data, soil types and inundated fractions/surfaces. A divergent point is how nitrogen pool is calculated.



We consider it as being produced by the organic matter mineralization and maximum nitrification. Whereas the other models compute it from nitrogen deposition. Moreover, they also take natural vegetation, swamps delineation (O-CN) and land cover as input data while we only focus on wetland types. These models assess N_2O emissions based on the processes of the nitrogen cycle such as denitrification. Our model apprehends denitrification as a function of carbon and nitrate contents (DOC , POC and NO_3) and inundated surfaces (SWAF). As a result, these models do not fully distinguish the alluvial floodplain from other lands (Xu et al., 2017) and underestimate its effects (Ito and Inatomi, 2012). Thus our results bring us to conclude that current physically-based N_2O emissions models are likely to slightly underestimate the contribution of wetlands in the global budget.

4.3 Wetlands and integrated ecosystem emissions

In this section, our model outputs for wetlands emissions are compared to local in situ measurements of the ecosystem N_2O and CO_2 emissions. Table 4 summarizes the different results from in situ measurements for N_2O and CO_2 and the closest simulation node from our simulation. When comparing the N_2O with in situ campaigns performed by (Koschorreck, 2005) and (Keller et al., 2005) at Manaus plateau and Santarem, the wetlands emissions from this study are roughly 1/200 of the integrated ecosystem observed emissions. CO_2 emissions at local in situ measurements (Keller et al., 2005) as well as to broader measurements (Richey et al., 2002) are compared to our models outputs. Our wetlands estimations are critically lower (10^4) than integrated ecosystem observations. As expected, even though CO_2 emissions from wetland denitrification are about 2.16×10^9 kgC- CO_2 per year over the Amazon basin, these emissions are negligible when compared to the full ecosystem Carbon emissions (Cole et al., 2007; Davidson et al., 2010). Overall, CO_2 emissions from denitrification over the whole Amazon basin participate to 0.01% of the carbon emissions of the watershed. Most of the CO_2 emissions over the Amazon are attributed to processes such as organic matter respiration from biomass. Confirming previous studies, this result means that even a small change in the distribution of wetlands cover over the Amazonian basin may drastically modify the carbon budget. It constitutes a topical subject for the Amazonian basin.

Table 4. Comparison of the values estimated by our study and the literature from the emissions of CO_2 and N_2O .

Paper	Gaz measured	Site	Ecosystem in situ obs.	Modeled wetlands	Units
Koschorreck (2005)	N_2O	Manaus plateau	$5 \pm 7.5 \times 10^6$	$2.4 \pm 1.1 \times 10^4$	gN/km ² /yr
Keller et al. (2005)	N_2O	Santarem	$8.6 \pm 0.7 \times 10^6$	$5.2 \pm 0.9 \times 10^4$	gN/km ² /yr
Richey et al. (2002)	CO_2	Amazon River wetlands	$6 \pm 0.3 \times 10^7$	$4.4 \pm 2.5 \times 10^3$	gC/km ² /yr
Keller et al. (2005)	CO_2	Santarem	$5.7 \pm 0.6 \times 10^7$	$1.6 \pm 0.9 \times 10^3$	gC/km ² /yr

4.4 The Amazonian wetlands emissions versus Tropical and temperate wetlands

We put in perspective the Amazonian wetlands emissions to a variety of wetland ecosystems such as the Congo basin, rice paddies of south-eastern Asia, the Garonne (France) and the Rhine (Europe) rivers with each possessing peculiar features.



The Congo basin can be considered, like the Amazon, as a pristine ecosystem regarding agricultural nitrogen inputs. On the contrary, rice paddies regions are territories with intensive agricultural activities, high nitrate fertilization and undergo several flooding events per year. Both the Congo basin and the rice paddies regions are part of the tropical region, like the Amazon basin. The N_2O emissions from the Amazon and the Congo basins are close. Our results for the Amazon and the ones exposed in Tian et al. (2018) for the Congo show emissions of $0.18 \text{ gN/m}^2/\text{yr}$. The two watersheds are pristine from agricultural nitrogen inputs and located toward the same latitudes, so relatively similar emissions of N_2O are expected. On the contrary, rice paddies shoot up with emissions of about $0.28 \text{ gN/m}^2/\text{yr}$. This is explained by the impacts of agricultural inputs and successive flooding on wetland ecosystems that increase the amount of greenhouse gases. The Garonne and the Rhine rivers catchments are in temperate regions under high agricultural pressures. The Garonne river, one of the main fluvial systems in France, is 525 km long draining a $55\,000 \text{ km}^2$ area into the Atlantic Ocean. The large range of altitudes and slopes within the watershed leads to a diversity of hydrological behaviours. The typical alluvial plain starts from its middle section and is about 4 km wide. The riparian forest and poplar plantations cover the first 50-200 m from the riverbank, beyond which lies agricultural land that accounts for 75% of the total area. The Rhine river, one of the main fluvial systems in Germany, is 1,233 km long draining a $198\,000 \text{ km}^2$ area from Switzerland to the North sea. The average denitrification reaches $132.52 \pm 3.9 \text{ kgN/ha/yr}$ Sun et al. (2017) and 653 kgN/ha/yr Sánchez-Perez et al. (1999) for the Garonne's and Rhine's floodplains respectively. The average rate of denitrification for the Amazon basin is $17.8 \pm 0.4 \text{ kgN/ha/yr}$ which is far less than values observed in European catchments. As a comparison the Òbidos - Manaus floodplain (table 2) denitrification potential is equivalent to the Garonne river. Overall, the Amazon wetland ecosystem can be regarded as a not-very active greenhouse gases emitting system compared to other ecosystems of the tropical region. Moreover, we may state that the Òbidos - Manaus floodplain possesses the same denitrification potential as a nitrate polluted temperate ecosystem.

4.5 Limitations of the current approach

The findings of this study have to be seen in light of some limitations. First, the sampling resolution of input data can induce bias. The SWAF product tends to underestimate water surface extents variability and land cover identification due to the coarse resolution of $25 \text{ km} \times 25 \text{ km}$. Second, the use of uniform k_{POC} and k_{DOC} values limits the capabilities of the model to fully consider the impact of the spatial variability of both geophysical and biological variables. Third, as highlighted by the present study, the lack of in situ measurements of N_2O emissions over tropical wetlands specifically increases the uncertainties and equifinalities for the calibration of model parameters and validation. Future studies should concentrate on: adding more remotely sensed geophysical variables at the adapted spatial resolution (Parrens et al., 2019), taking into account the fact that flooding actually sustains the different processes.

5 Conclusions

The main objective of the study is to quantify and assess CO_2 and N_2O emissions over the Amazonian wetlands during flooding periods. To achieve these goals we design a data driven methodology that relies on modelling and remote-sensing



products. It aims to estimate emissions linked to denitrification at large scale. The model parametrisation was justified by results from several published papers. It appears that denitrification mainly relies on *DOC* contents in the watershed. The study also contributes to better understand the functioning of the major floodplains of the Amazon Basin and their respective involvement in the Amazon Carbon and Nitrogen budget. It transpires that the most active floodplain is the Ôbidos-Manaus, which is responsible for the majority of processes. It may also be pointed out that each floodplain possesses its own functioning that depends on rainfalls and the hydrology of the floodplain's river. Overall, the results appear quite close to other large scale models; especially for N_2O emissions. Key factors of denitrification for the Amazon Basin were identified in the study. Future studies will concentrate in extending the current approach to other tropical basins, needless to say that local observations will be paramount for the validation of such exercise and preferably over the same period of analysis. Data from future missions like SWOT will deliver water heights at 21 days global coverage, which will improve the results of such studies through the integration of surfaces and volume information.

Author contributions. Ahmad Al Bitar, Sabine Sauvage, Marie Parrens, José-Miguel Sanchez-Pérez and Jérémy Guilhen conceived and designed the methodology and the algorithms. Jérémy Guilhen performed the analysis. Jean-Michel Martinez, Gwenael Abril and Patricia Moreira-Turcq provided the scientific expertise and corrections to the manuscript. Jérémy Guilhen and Ahmad Al Bitar wrote the first draft. Marie Parrens did all the graphs. All authors wrote the final manuscript.

Competing interests. All co-authors declare that no competing interests are present

Acknowledgements. This work was funded by the Midi-Pyrénées' "Axe transversal cycle du Carbone, de l'Azote et gaz à effet de serre". The SWAF product was developed in the framework of the TOSCA SOLE and SWOT-downstream programs from CNES. We thank the HyBam observatory network for providing the data needed for this study.



References

- Abril, G. and Borges, A.: Carbon leaks from flooded land: do we need to re-plumb the inland water active pipe?, *Biogeoscience Discussions*, <https://doi.org/https://doi.org/10.5194/bg-2018-239>, 2018.
- Abril, G. and Frankignoulle, M.: Nitrogen–alkalinity interactions in the highly polluted scheldt basin (belgium), *Water Research*, 35, [https://doi.org/10.1016/S0043-1354\(00\)00310-9](https://doi.org/10.1016/S0043-1354(00)00310-9), 2001.
- 5 Abril, G., Martinez, J.-M., Artigas, L. F., Moreira-Turcq, P., Benedetti, M. F., Vidal, L., Meziane, T., Kim, J.-H., Bernardes, M. C., Savoye, N., Deborde, J., Souza, E. L., Alboric, P., Landim de Souza, M. F., and Roland, F.: Amazon River carbon dioxide outgassing fuelled by wetlands, *Nature*, 505, 395–398, <https://doi.org/10.1038/nature12797>, <https://www.nature.com/nature/journal/v505/n7483/full/nature12797.html>, 2014.
- 10 Al Bitar, A., Mialon, A., Kerr, Y. H., Cabot, F., Richaume, P., Jacquette, E., Quesney, A., Mahmoodi, A., Tarot, S., Parrens, M., et al.: The global SMOS Level 3 daily soil moisture and brightness temperature maps, *Earth System Science Data*, 9, 293–315, 2017.
- Birkett, C. M., Mertes, L., Dunne, T., Costa, M., and Jasinski, M.: Surface water dynamics in the Amazon Basin: Application of satellite radar altimetry, *Journal of Geophysical Research: Atmospheres*, 107, LBA–26, 2002.
- Borges, A. V., Abril, G., Darchambeau, F., Teodoru, C. R., Deborde, J., Vidal, L. O., Lambert, T., and Bouillon, S.: Divergent biophysical controls of aquatic CO₂ and CH₄ in the World's two largest rivers, *Scientific Reports*, 5, 15 614, <https://doi.org/10.1038/srep15614>, <http://www.nature.com/srep/2015/151023/srep15614/full/srep15614.html>, 2015.
- 15 Bourgoin, L. M., Bonnet, M.-P., Martinez, J.-M., Kosuth, P., Cochonneau, G., Moreira-Turcq, P., Guyot, J.-L., Vauchel, P., Filizola, N., and Seyler, P.: Temporal dynamics of water and sediment exchanges between the Curuaó floodplain and the Amazon River, Brazil, *Journal of Hydrology*, 335, 140–156, <https://doi.org/10.1016/j.jhydrol.2006.11.023>, <http://www.sciencedirect.com/science/article/pii/S0022169406005932>, 2007.
- 20 Bréon, F.-M. and Ciais, P.: Spaceborne remote sensing of greenhouse gas concentrations, *Comptes Rendus Geoscience*, 342, 412–424, 2010.
- Brettar, I., Sanchez-Perez, J., and Tremolières, M.: Nitrate elimination by denitrification in hardwood forest soils of the Upper Rhine floodplain – correlation with redox potential and organic matter, *Hydrobiologia*, 469, 11–21, <https://doi.org/10.1023/A:1015527611350>, 2002.
- Callode, J., Cochonneau, G., Alves, F., Guyot, J.-L., Guimarães, V., and De Oliveira, E.: Les apports en eau de l'Amazonie à l'Océan Atlantique, *Revue des sciences de l'eau*, *Revue des sciences de l'eau*, 23, 247–273, <https://doi.org/10.7202/044688ar>, <http://www.erudit.org/fr/revues/rseau/2010-v23-n3-n3/044688ar/>, 2010.
- 25 Ciais, P. and Coauthors.: Carbon and other biogeochemical cycles., *Climate Change 2013: The Physical Science Basis. Contribution of Working Group I to the Fifth Assessment Report of the Intergovernmental Panel on Climate Change*, 2013.
- Cole, J. J., Prairie, Y. T., Caraco, N. F., McDowell, W. H., Tranvik, L. J., Striegl, R. G., Duarte, C. M., Kortelainen, P., Downing, J. A., Middelburg, J. J., and Melack, J.: Plumbing the Global Carbon Cycle: Integrating Inland Waters into the Terrestrial Carbon Budget, *Ecosystems*, 10, 172–185, <https://doi.org/10.1007/s10021-006-9013-8>, <https://link.springer.com/article/10.1007/s10021-006-9013-8>, 2007.
- 30 Davidson, E. A., Figueiredo, R. O., Markewitz, D., and Aufdenkampe, A. K.: Dissolved CO₂ in small catchment streams of eastern Amazonia: A minor pathway of terrestrial carbon loss, *Journal of Geophysical Research: Biogeosciences*, 115, G04 005, <https://doi.org/10.1029/2009JG001202>, <http://onlinelibrary.wiley.com/doi/10.1029/2009JG001202/abstract>, 2010.
- 35 de Fatima F. L. Rasera, M., Ballester, M. V. R., Krusche, A. V., Salimon, C., Montebelo, L. A., Alin, S. R., Victoria, R. L., and Richey, J. E.: Estimating the Surface Area of Small Rivers in the Southwestern Amazon and Their Role in CO₂ Outgassing, *Earth Interactions*, 12, 1–16, <https://doi.org/10.1175/2008EI257.1>, <http://journals.ametsoc.org/doi/abs/10.1175/2008EI257.1>, 2008.



- de Freitas, H. A., Pessenda, L. C. R., Aravena, R., Gouveia, S. E. M., de Souza Ribeiro, A., and Boulet, R.: Late Quaternary Vegetation Dynamics in the Southern Amazon Basin Inferred from Carbon Isotopes in Soil Organic Matter, *Quaternary Research*, 55, 39–46, <https://doi.org/10.1006/qres.2000.2192>, <http://www.sciencedirect.com/science/article/pii/S0033589400921926>, 2001.
- Devol, A. H., Forsberg, B. R., Richey, J. E., and Pimentel, T. P.: Seasonal variation in chemical distributions in the Amazon (Solimoes) River: A multiyear time series, *Global Biogeochemical Cycles*, 9, 307–328, <https://doi.org/10.1029/95GB01145>, <http://onlinelibrary.wiley.com/doi/10.1029/95GB01145/abstract>, 1995.
- Dodla, S. K., Wang, J. J., DeLaune, R. D., and Cook, R. L.: Denitrification potential and its relation to organic carbon quality in three coastal wetland soils, *Science of The Total Environment*, 407, 471–480, <https://doi.org/10.1016/j.scitotenv.2008.08.022>, <http://www.sciencedirect.com/science/article/pii/S0048969708008395>, 2008.
- Engelen, R. J., Serrar, S., and Chevallier, F.: Four-dimensional data assimilation of atmospheric CO₂ using AIRS observations, *Journal of Geophysical Research: Atmospheres*, 114, 2009.
- Goldman, A. E., Graham, E. B., Crump, A. R., Kennedy, D. W., Romero, E. B., Anderson, C. G., Dana, K. L., Resch, C. T., Fredrickson, J. K., and Stegen, J. C.: Carbon cycling at the aquatic-terrestrial interface is linked to parafluvial hyporheic zone inundation history, *Biogeosciences Discuss.*, 2017, 1–20, <https://doi.org/10.5194/bg-2017-28>, <http://www.biogeosciences-discuss.net/bg-2017-28/>, 2017.
- Hulme, P. E.: Adapting to climate change: is there scope for ecological management in the face of a global threat?, *Journal of Applied Ecology*, 42, 784–794, <https://doi.org/10.1111/j.1365-2664.2005.01082.x>, <http://onlinelibrary.wiley.com/doi/10.1111/j.1365-2664.2005.01082.x/abstract>, 2005.
- Ito, R. and Inatomi, M.: Use of a process-based model for assessing the methane budgets of global terrestrial ecosystems and evaluation of uncertainty., *Biogeosciences*, 9, 759–773, <https://doi.org/10.5194/bg-9-759-2012>, 2012.
- Johnson, K., Riser, S., and Ravichandran, M.: Oxygen Variability Controls Denitrification in the Bay of Bengal Oxygen Minimum Zone, *Geophysical Research Letters*, 46, <https://doi.org/10.1029/2018GL079881>, 2019.
- Keller, M., Varner, R., Dias, J. D., Silva, H., Crill, P., de Oliveira, R. C., and Asner, G. P.: SoilAtmosphere Exchange of Nitrous Oxide, Nitric Oxide, Methane, and Carbon Dioxide in Logged and Undisturbed Forest in the Tapajos National Forest, Brazil, *Earth Interactions*, 9, 1–28, <https://doi.org/10.1175/EI125.1>, <http://journals.ametsoc.org/doi/abs/10.1175/EI125.1>, 2005.
- Kerr, Y. H., Waldteufel, P., Wigneron, J. P., Delwart, S., Cabot, F., Boutin, J., Escorihuela, M. J., Font, J., Reul, N., Gruhier, C., Juglea, S. E., Drinkwater, M. R., Hahne, A., Martin-Neira, M., and Mecklenburg, S.: The SMOS Mission: New Tool for Monitoring Key Elements of the Global Water Cycle, *Proceedings of the IEEE*, 98, 666–687, <https://doi.org/10.1109/JPROC.2010.2043032>, 2010.
- Korol, A., Noe, G., and Ahn, C.: Controls of the spatial variability of denitrification potential in nontidal floodplains of the Chesapeake Bay watershed, USA, *Geoderma*, 338, <https://doi.org/10.1016/j.geoderma.2018.11.015>, 2019.
- Koschorreck, M.: Nitrogen Turnover in Drying Sediments of an Amazon Floodplain Lake, *Microbial Ecology*, 49, 567–577, <https://doi.org/10.1007/s00248-004-0087-6>, <https://link.springer.com/article/10.1007/s00248-004-0087-6>, 2005.
- Koschorreck, M. and Darwich, A.: Nitrogen dynamics in seasonally flooded soils in the Amazon floodplain, *Wetlands Ecology and Management*, 11, 317–330, <https://doi.org/10.1023/B:WETL.0000005536.39074.72>, <https://link.springer.com/article/10.1023/B:WETL.0000005536.39074.72>, 2003.
- Lauerwald, R., Regnier, P., Camino-Serrano, M., Guenet, B., Guimberteau, M., Ducharne, A., Polcher, J., and Ciais, P.: ORCHILEAK (revision 3875): a new model branch to simulate carbon transfers along the terrestrial–aquatic continuum of the Amazon basin, *Geosci. Model Dev.*, 10, 3821–3859, <https://doi.org/10.5194/gmd-10-3821-2017>, 2017.
- Legros, J.-P.: *Les grands sols du monde*, PPUR presses polytechniques, 2007.



- Lloyd, J., Kolle, O., Fritsch, H., De Freitas, S. R., Silva Dias, M. A. F., Artaxo, P., Nobre, A. D., De Araujo, A. C., Kruijt, B., Sogacheva, L., Fisch, G., Thielmann, A., Kuhn, U., and Andreae, M. O.: An airborne regional carbon balance for Central Amazonia, *Biogeosciences*, 4, 759–768, <https://hal.archives-ouvertes.fr/hal-00297719>, 2007.
- Ludwig, W., Probst, J.-L., and Kempe, S.: Predicting the oceanic input of organic carbon by continental erosion, *Global Biogeochemical Cycles*, 10, 23–41, <https://doi.org/10.1029/95GB02925>, <http://onlinelibrary.wiley.com/doi/10.1029/95GB02925/abstract>, 1996.
- Martinez, J.-M. and Le Toan, T.: Mapping of flood dynamics and spatial distribution of vegetation in the Amazon floodplain using multitemporal SAR data, *Remote sensing of Environment*, 108, 209–223, 2007.
- Moreira-Turcq, P., Bonnet, M.-P., Amorim, M., Bernardes, M., Lagane, C., Maurice, L., Perez, M., and Seyler, P.: Seasonal variability in concentration, composition, age, and fluxes of particulate organic carbon exchanged between the floodplain and Amazon River, *Global Biogeochemical Cycles*, 27, 119–130, <https://doi.org/10.1002/gbc.20022>, <http://onlinelibrary.wiley.com/doi/10.1002/gbc.20022/abstract>, 2013.
- Paiva, R. C. D., Collischonn, W., and Buarque, D. C.: Validation of a full hydrodynamic model for large-scale hydrologic modelling in the Amazon, *Hydrological Processes*, 27, 333–346, <https://doi.org/10.1002/hyp.8425>, <http://onlinelibrary.wiley.com/doi/10.1002/hyp.8425/abstract>, 2013.
- Parrens, M., Al Bitar, A., Frappart, F., Papa, F., Calmant, S., Crotaux, J.-F., Wigneron, J.-P., and Kerr, Y.: Mapping Dynamic Water Fraction under the Tropical Rain Forests of the Amazonian Basin from SMOS Brightness Temperatures, *Water*, 9, 350, <https://doi.org/10.3390/w9050350>, <http://www.mdpi.com/2073-4441/9/5/350>, 2017.
- Parrens, M., Al Bitar, A., Frappart, F., Paiva, R., Wongchuig, S., Papa, F., Yamasaki, D., and Kerr, Y.: High resolution mapping of inundation area in the Amazon basin from a combination of L-band passive microwave, optical and radar datasets, *International Journal of Applied Earth Observation and Geoinformation*, 81, <https://doi.org/10.1016/j.jag.2019.04.011>, 2019.
- Pekel, J.-F., Cottam, A., Gorelick, N., and Belward, A. S.: High-resolution mapping of global surface water and its long-term changes, *Nature*, 540, 418, 2016.
- Peter, S., Koetzsch, S., Traber, J., Bernasconi, S., Wehrli, B., and Durisch-Kaiser, E.: Intensified organic carbon dynamics in the ground water of a restored riparian zone, *Freshwater Biology*, 57, <https://doi.org/10.1111/j.1365-2427.2012.02821.x>, 2012.
- Peyrard, D., Delmotte, S., Sauvage, S., Namour, P., Gorino, M., Vervier, P., and Sanchez-Porez, J.-M.: Longitudinal transformation of nitrogen and carbon in the hyporheic zone of an N-rich stream: A combined modelling and field study, *Physics and Chemistry of the Earth*, vol. 36, pp. 599–611, <http://dx.doi.org/10.1016/j.pce.2011.05.003>, 2010.
- Richey, J. E., Hedges, J. I., Devol, A. H., Quay, P. D., Victoria, R., Martinelli, L., and Forsberg, B. R.: Biogeochemistry of carbon in the Amazon River, *Limnology and Oceanography*, 35, 352–371, <https://doi.org/10.4319/lo.1990.35.2.0352>, <http://onlinelibrary.wiley.com/doi/10.4319/lo.1990.35.2.0352/abstract>, 1990.
- Richey, J. E., Melack, J. M., Aufdenkampe, A. K., Ballester, V. M., and Hess, L. L.: Outgassing from Amazonian rivers and wetlands as a large tropical source of atmospheric CO₂, *Nature*, 416, 617–620, <https://doi.org/10.1038/416617a>, 2002.
- Russell, M., Fulford, R., Murphy, K., Lane, C., Harvey, J., Dantin, D., Alvarez, F., Nestlerode, J., Teague, A., Harwell, M., and Almario, A.: Relative Importance of Landscape Versus Local Wetland Characteristics for Estimating Wetland Denitrification Potential, *Wetlands*, 39, <https://doi.org/10.1007/s13157-018-1078-6>, 2019.
- Scofield, V., Melack, J. M., Barbosa, P. M., Amaral, J. H. F., Forsberg, B. R., and Farjalla, V. F.: Carbon dioxide outgassing from Amazonian aquatic ecosystems in the Negro River basin, *Biogeochemistry*, 129, 77–91, <https://doi.org/10.1007/s10533-016-0220-x>, <https://link.springer.com/article/10.1007/s10533-016-0220-x>, 2016.



- Sun, X., Bernard-Jannin, L., Sauvage, S., Garneau, C., Arnold, J., Srinivasan, R., and Sánchez-Perez, J.: Assessment of the denitrification process in alluvial wetlands at floodplain scale using the SWAT model., *Ecological Engineering*, 103, 344 – 358, <https://doi.org/10.1016/j.ecoleng.2016.06.098>, 2017.
- Sánchez-Perez, J., Tremolières, M., Takatert, N., Ackerer, P., Eichhorn, A., and Maire, G.: Quantification of nitrate removal by a flooded alluvial zone in the Ill floodplain (Eastern France)., *Hydrobiologia*, 410, 185–193, <https://doi.org/10.1023/A:1003834014908>, 1999.
- Sánchez-Pérez, J., Vervier, P., Garabétian, F., Sauvage, S., Loubet, M., Rols, J., Bariac, T., and Weng, P.: Nitrogen dynamics in the shallow groundwater of a riparian wetland zone of the Garonne, SW France: nitrate inputs, bacterial densities, organic matter supply and denitrification measurements, *Hydrology and Earth System Sciences*, 7, <https://doi.org/https://doi.org/10.5194/hess-7-97-2003>, 2003.
- Tian, H., Yang, J., Lu, C., Xu, R., Canadell, J., Jackson, R., Arneeth, A., Chen, J., Chen, G., Ciais, P., Gerber, S., Ito, A., Huang, Y., Joos, F., Lienert, S., Messina, P., Olin, S., Pan, S., Peng, C., Saikawa, E., Thompson, R., Vuivhard, N., Winiwarter, W., Zaehle, S., Zhang, B., Zhang, K., and Zhu, Q.: The global N₂O Model Intercomparison Project (NMIP): Objectives, Simulation Protocol and Expected Products., *Bulletin of the American Meteorological Society*, <https://doi.org/10.1175/BAMS-D-17-0212.1>, 2018.
- Xu, R., Tian, H., Lu, C., Pan, S., Chen, J., Yang, J., and Zhang, B.: Preindustrial nitrous oxide emissions from the land biosphere estimated by using a global biogeochemistry model., *Clim. Past*, 13, 977–990, <https://doi.org/10.5194/cp-13-977-2017>, 2017.
- Zaehle, S. and Friend, A.: Carbon and nitrogen cycle dynamics in the O-CN land surface model: 1. Model description, site-scale evaluation, and sensitivity to parameter estimates., *Global Biogeochemical Cycles*, 24, <https://doi.org/10.1029/2009GB003521>, 2010.